Chapter 2

Interfacial Engineering of Flexible Transparent Conducting Films

Joong Tark Han and Geon-Woong Lee

Additional information is available at the end of the chapter

http://dx.doi.org/10.5772/intechopen.80259

Abstract

One-dimensional (1D) carbon nanotubes (CNTs) and silver nanowires (AgNWs) have been used as replacements for brittle indium tin oxide (ITO) in the fabrication of transparent conducting films (TCFs), which can be used in opto-electronic devices such as screen panels, solar cell panels, and organic light-emitting diodes. This chapter describes a fabrication method of high-performance TCFs by solution processing of single-walled CNTs (SWCNTs) and AgNWs. Highly uniform TCFs with SWCNTs and AgNW inks were fabricated using spray deposition. Their performance was modulated by interfacial engineering such as overcoating with silane compound for densification of SWCNT networks and chemical or photothermal welding of SWCNT networks on thermoplastic substrates. Moreover, the hybridization of SWCNTs, AgNWs, and graphene oxide nanosheets is a promising approach to mitigate their drawbacks via p-type doping, electrical stabilization, or interfacial stabilization on plastic substrates. The rational control of 1D material networks can provide a good opportunity to fabricate high-performance TCFs for flexible opto-electronic devices.

Keywords: single-walled carbon nanotubes, silver nanowires, interfacial engineering, graphene oxide, dispersion, sheet resistance

1. Introduction

One-dimensional (1D) conducting nanomaterials such as carbon nanotubes (CNTs) and metal nanowires have been studied to replace brittle indium tin oxide (ITO) films for flexible opto-electronic devices because of their flexibility and high electrical conductivity as well as solution processability [1–5]. There are growing needs for high-performance transparent conducting films (TCFs) with flexibility to realize flexible displays or solar cells. Solution processing of conducting nanomaterials for TCFs has many challenging issues in order to

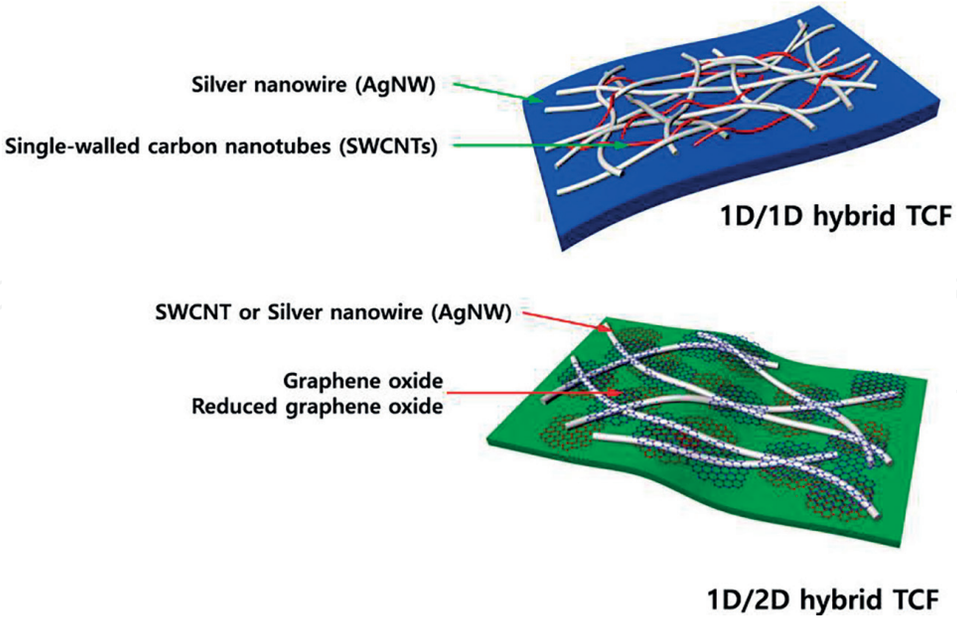

Figure 1. Scheme of hybrid TCFs fabricated with 1D/1D hybrid materials and 1D/2D hybrid materials by solution processing.

achieve high performance, including the intrinsic properties of the materials, the dispersion of nanomaterials, and interfacial engineering of coating films on plastic substrates. Moreover, to mitigate the drawbacks of each conducting nanomaterial, we need a rational hybridization strategy to achieve the fabrication of high performance TCFs on plastic substrates (**Figure 1**).

Therefore, this chapter describes some of the research on the fabrication of high-performance TCFs based on single-walled CNTs (SWCNTs) and silver nanowires (AgNWs) over the past 8 years that addresses these and other challenges, with an emphasis on our own efforts. We begin with the realization of TCFs with high uniformity by spray deposition and then describe the interfacial engineering of TCFs on plastic substrates. Furthermore, we describe the fabrication of flexible TCFs with 1D/1D hybrid structures and 1D/2D hybrid materials with SWCNTs and AgNWs as 1D materials and graphene oxide as a 2D material. We conclude with some discussion of future directions and the remaining challenges in chemically exfoliated graphene technologies.

2. Fabrication of TCFs by spray coating

Spray coating methods can be used to fabricate flexible TCFs with aqueous single-walled carbon nanotube (SWCNT) solutions or silver nanowire (AgNW) solutions on plastic substrates. As shown in **Figure 2**, thin films were deposited on the substrate by the atomization of aqueous solution using high-pressure nitrogen gas through a spray nozzle. The gas flow rate, nozzle height, and pitch should be controlled to fabricate uniform films with high opto-electrical performance. As a model system, SWCNT solution dispersed in aqueous surfactant and aqueous AgNW solution containing a small amount (0.01 wt%) of polyvinylpyrrolidone (PVP) were used to investigate the spreading behavior on surface energy-controlled substrates. To control the surface energy of the substrate, plastic substrates were irradiated with UV-ozone (UVO). The wettability of coating inks is critical for fabrication of uniform films by spraying. **Figure 3**

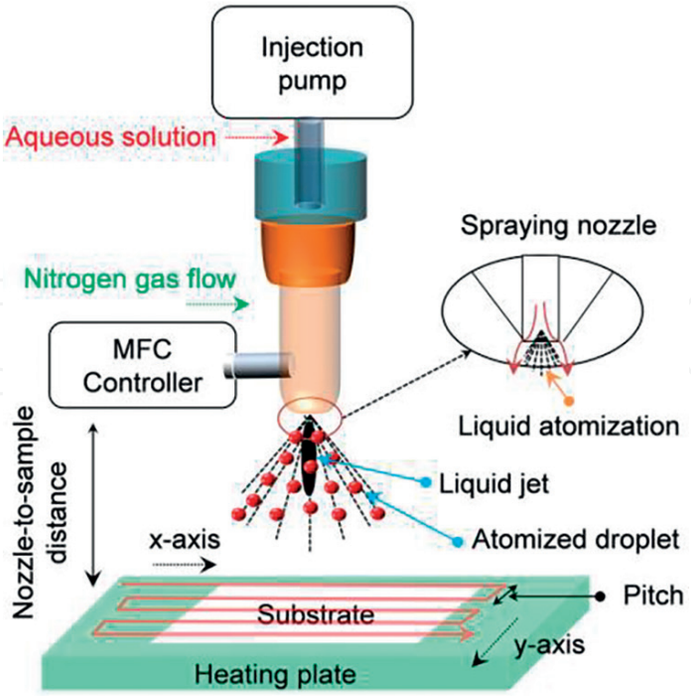

Figure 2. Schematic of the automatic spray coating system with mass flow controller, injection pump, and atomizing nozzle. The X- and Y-direction can be controlledautomatically by robotics [6].

shows the contact angle (CA) change with an increase in UVO irradiation time of polycarbonate substrates. The CA of the SWCNT/surfactant solution decreases from 15 to 10°. The CA of the aqueous AgNW solution decreases from 68.7 to 36.6° with an increasing UVO irradiation time, and the size of the deposited liquid droplet increases from 8 to 13 mm. The nozzle height and the spraying pitch were optimized to 70 and 7 mm, respectively.

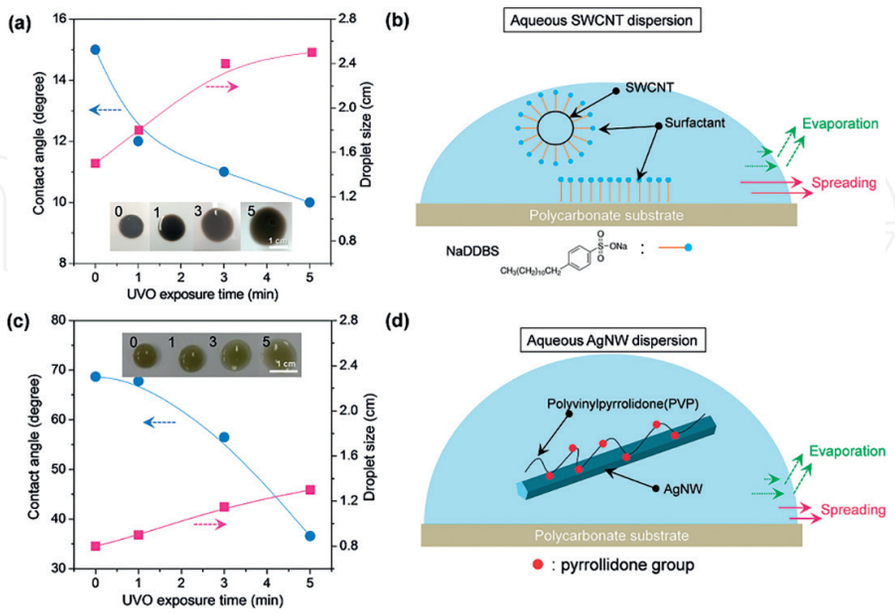

Figure 3. Contact angles and spread droplet sizes of (a) the aqueous SWCNT solution dispersed by sodium dodecylbenzene sulfonate and (c) the aqueous AgNW solution containing PVP on polycarbonate substratesby varying the UVO exposure time. The inset photoimages in (a) and (c) show the spread SWCNT and AgNW droplet sizes on the substrate by varying the UVO-irradiation time indicated by values. (b) and (d) Schematics of spreading of the SWCNT (b) and AgNW (d) droplets on substrates [6].

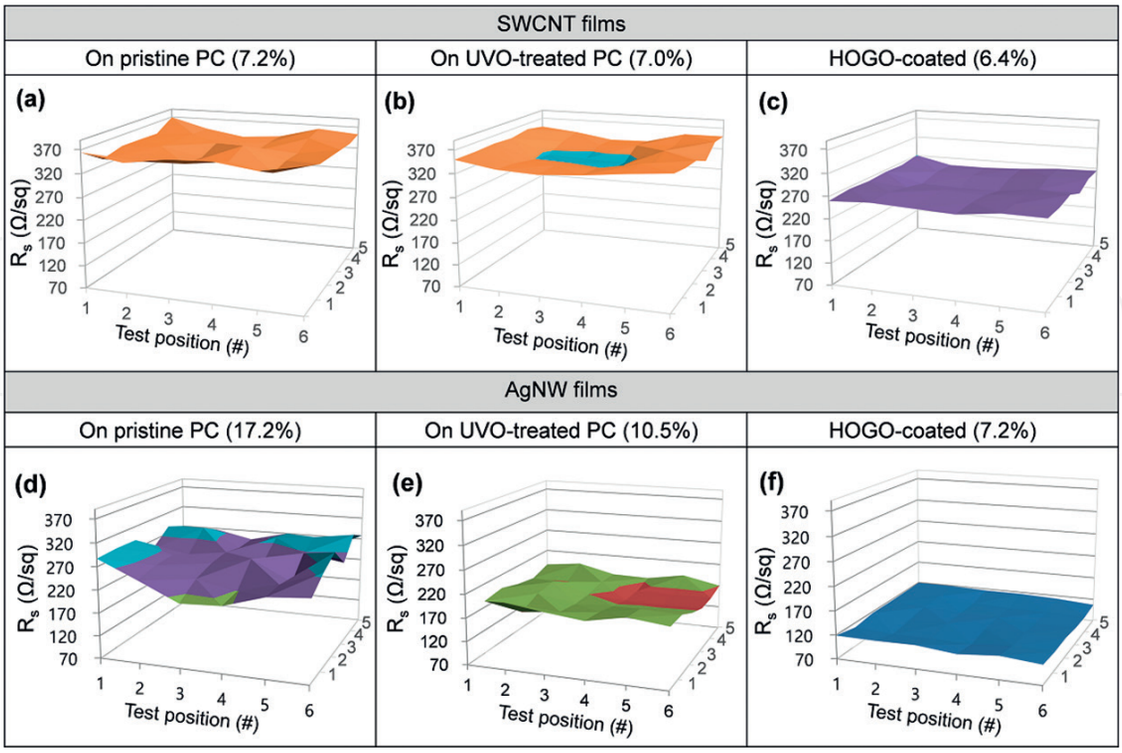

Figure 4. The sheet resistance (R_s) uniformity of (a–c) the SWCNT films and (d–f) the AgNW films on (a, d) pristine polycarbonate (PC), (b, e) UVO-irradiated PC substrates, and (c, f) after graphene oxide (HOGO) coating of the conducting films fabricated on UVO-treated substrates [6].

Another way to enhance the uniformity of the films is deposition of hydrophilic graphene oxide (GO) nanosheets onto the substrate. **Figure 4** shows the sheet resistance (R_s) distribution of the SWCNT and the AgNW films spray-coated on surface energy-controlled substrates and after deposition of GO nanosheets onto the films. After UVO treatment, the R_s uniformity of AgNW films was dramatically improved and reached 7.2%, resulting in T = 98% and R_s = 100 Ω/sq for the highlyoxidized GO (HOGO)-coated AgNW films.

3. Interfacial engineering for high-performance TCFs

3.1. Modulation of the sheet resistance of SWCNT-based TCFs by silane sol

In this study, we investigated the effect of the interfacial tension between bare SWCNT network films and a top-coating of passivation materials on the R_s of the film. We demonstrated that the R_s of the SWCNT film can be affected by a thermal expansion coefficient (CTE) mismatch between the substrate and the SWCNT film.

The spray-coated SWCNT films have porous structures on a scale of tens of nanometers. The R_s and transmittance are related by [7].

$$T(\lambda) = \left(1 + \frac{188.5}{R_s}\frac{\sigma_{Op}(\lambda)}{\sigma_{DC}}\right)^{-2}, \quad (1)$$

where σ_{DC} and σ_{Op} are the DC and optical conductivities, respectively.

The conductivity, σ_{DC}, of the disordered nanotube films depends on the number density of the network junctions, N_J, which in turn scales with the network morphology through the film fill-factor, V_f, the mean diameter, $<D>$, of the bundles, and the mean junction resistance, $<R_J>$ [8–11],

$$\sigma_{DC} = \frac{K}{< R_J >} \frac{V_f^2}{< D >^3} \quad (2)$$

Here, K is the proportionality factor that scales with the bundle length. Therefore, if we can reduce $<R_J>$ and V_f, the sheet resistance of the SWCNT films can be improved. To realize this, the SWCNT films were coated with silane sols by considering their surface energy. Considering the interfacial tension between the SWCNT film and silane sols, two top-coating materials such as a tetraorthosilicate (TEOS) sol with silanol groups and methyltrimethoxysilane (MTMS) sol with hydrophobic methyl groups were used. It is worth noting that top-coating with TEOS sol unexpectedly decreased the R_s of the film to less than 80% of the R_s of the as-prepared film. However, the R_s values of MTMS sol-coated SWCNT films gradually increased. This large disparity between MTMS and TEOS sols can be explained by a change in the contact resistance between the bundles. Hydrophilic TEOS sol can densify the hydrophobic SWCNT networks, while MTMS sol, having methyl groups, can penetrate the hydrophobic SWCNT networks, resulting in an increase of the contact resistance of SWCNTs. This interfacial tension effect was minimized by deposition of gold chloride solution onto the SWCNT film (**Figure 5b**) to make it hydrophilic, as shown in **Figure 5c**.

Figure 6 shows the R_s change after heating at 130°C and cooling. Bare PET, hard-coated PET, and glass substrates were used to illustrate the CTE mismatch effect on the R_s changes of SWCNT films. Interestingly, the R_s of the SWCNTs on bare PET substrates increased by 40% relative to the initial values, while the R_s increase was suppressed in bare SWCNT films on hard-coated PET and glass. These results imply that the CTE value should be considered in order to obtain highly stable SWCNT TCFs on plastic substrates. To illustrate this phenomenon, a Raman spectroscopic study was performed, and the G+ and G− peak positions related to the strain of SWCNTs were compared. The G-band frequencies for SWCNT films on bare PET were up-shifted by 1–2 cm^{-1} after heating at 130°C and cooling, which corresponds to a

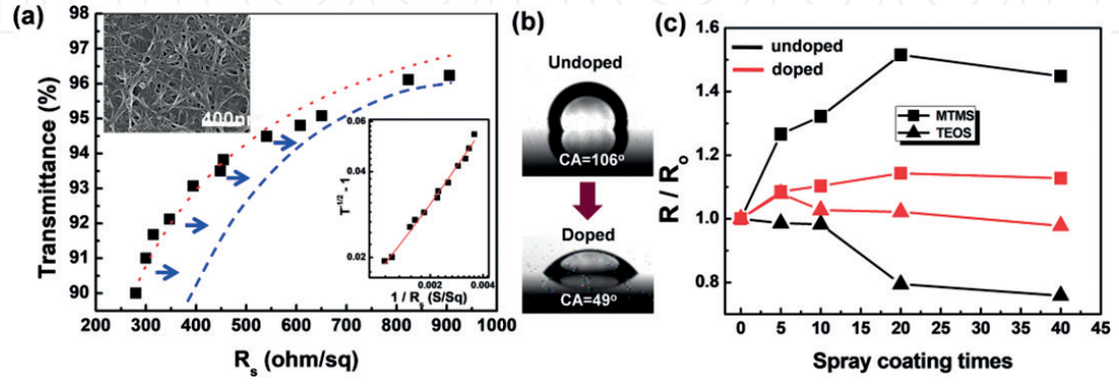

Figure 5. (a) The R_s versus transmittance plot of SWCNT film deposited by spraying on PET substrates. (b) Wettability of pristine SWCNT film and SWCNT filmdoped with gold chloride. (c) The R_s change of pristine and doped SWCNT films by varying spray coating times of top-coating materials (methyl trimethoxysilane (MTMS) sol, tetraethoxysilane (TEOS) sol) after baking at 80°C for 1 h [12].

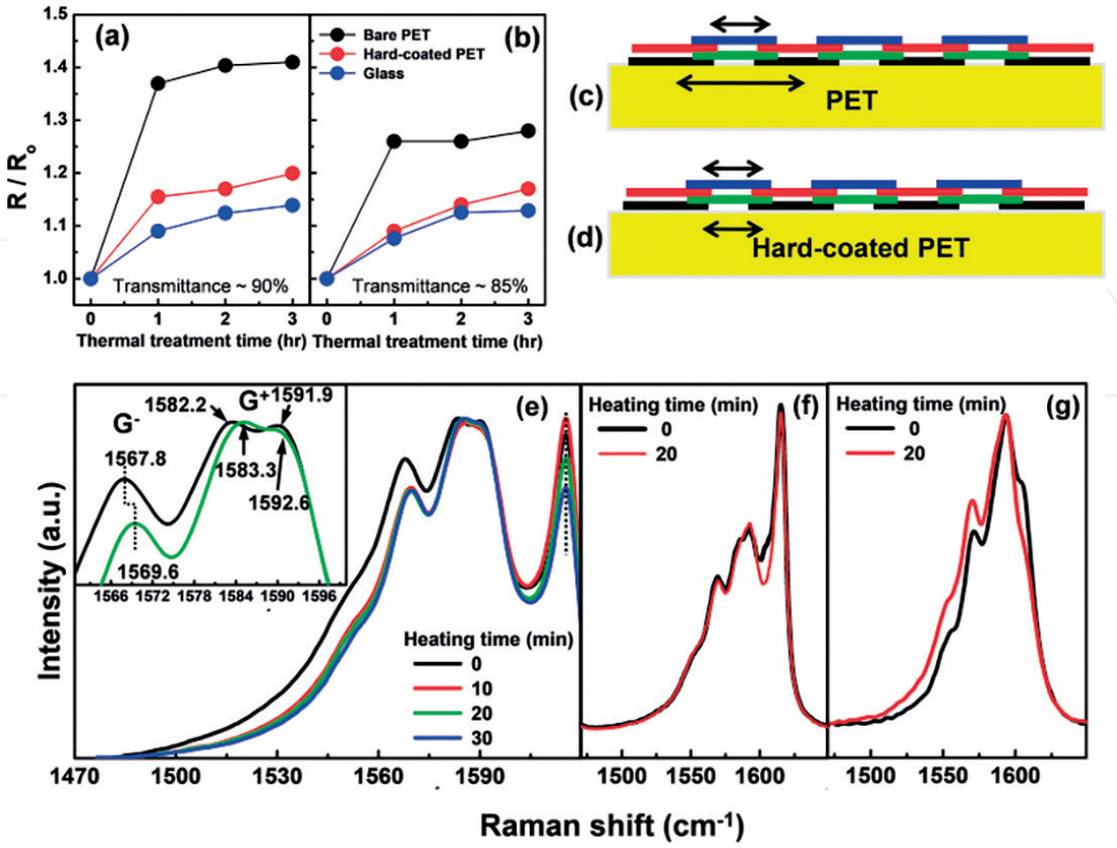

Figure 6. (a, b) The R_s changes of SWCNT films with different transmittance values, after heating at 130°C, as a function of thermal treatment time. (c, d) Scheme of thermal expansion mismatch between the SWCNT layers and bare PET or hard-coated PET after heating and cooling. (e–g) Raman spectra (G band) of SWCNT films fabricated on (e) bare PET, (f) hard-coated PET, and (g) glass after heating at 130°C for 20 min, followed by cooling [12].

compressive strain of ~0.1%. This compressive strain may cause the increase of the R_s of the SWCNT film on bare PET.

3.2. Self-passivation of SWCNT films on plastic substrates by nanowelding

Plastic substrates are generally used to fabricate flexible TCFs by deposition of CNTs or metal nanowires. In particular, the electrical properties of SWCNT network films are sensitive to humidity and temperature. In this context, top-coating with passivation materials or hybridization with binder materials are applicable for improving the stability of TCFs. Another way to passivate TCFs is welding or embedding in plastic substrates by chemical or thermal treatments. **Figure 7** shows the R_s change of the SWCNT films after deposition of solvents. To investigate the solvent effects, we used solvents with optimal polarity and affinity for the PET substrate. Moreover, the presence of electron-donating and electron-withdrawing groups in the solvent molecules can affect the electronic structure of the SWCNTs. Thus, nonpolar solvents were selected. In particular, aromatic hydrocarbon, benzene, and toluene can swell the PET substrate. Most interestingly, deposition of toluene or benzene decreased the R_s of the SWCNT films. After doping with gold chloride, the R_s and transmittance of the film were measured to be 85 Ω/sq and 90%, respectively. Moreover, I-V plots measured after solvent

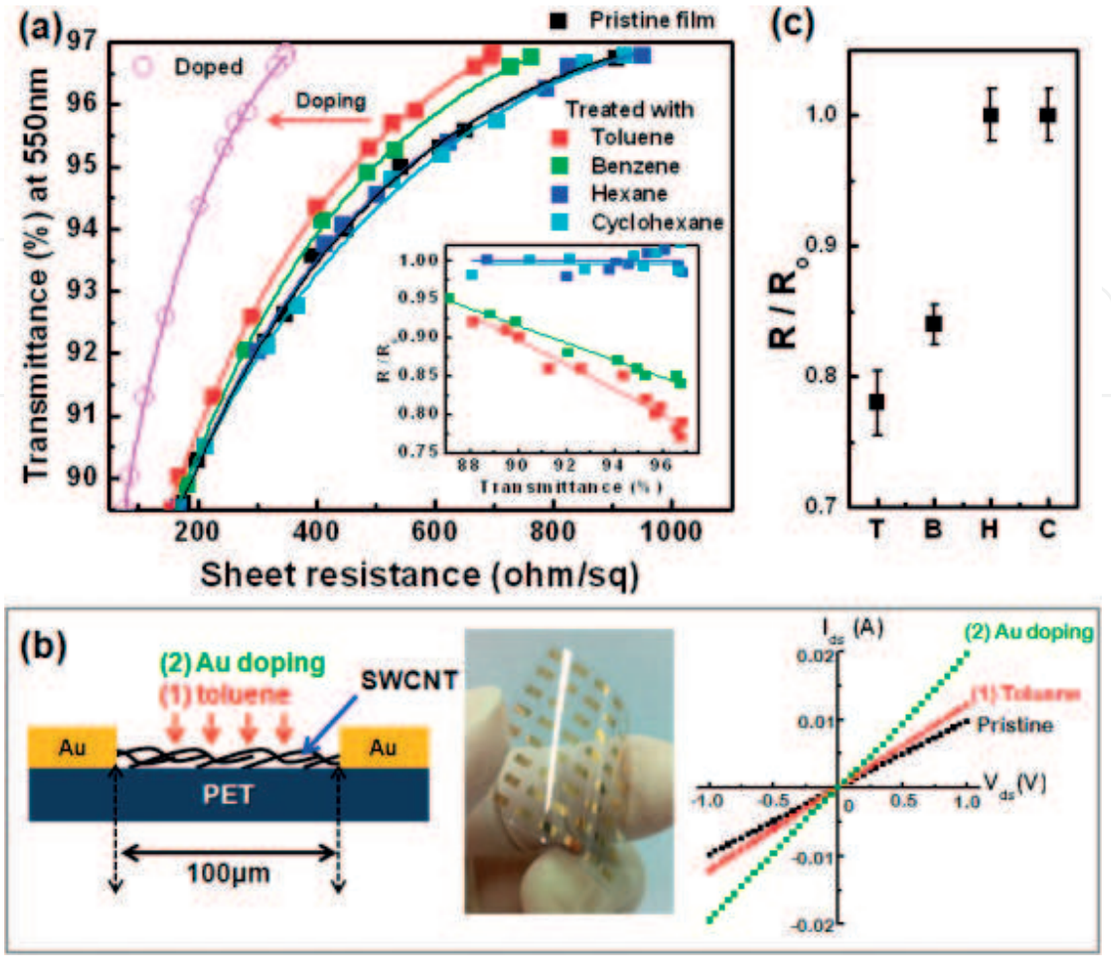

Figure 7. (a) R_s versus transmittance plots for pristine SWCNT films prepared from a SWNT/SDBS solution on PET surfaces, and after deposition of solvents and dopants. (b) In-situ conductivity measurements of SWCNT films after deposition of toluene and gold chloride. (c) R_s changes of bare SWCNT films in comparison with the same films treated with solvents: toluene (T), benzene (B), hexane (H), and cyclohexane (C) [13].

deposition show clearly that the electrical conductivity of the SWCNT films was enhanced after toluene deposition, which can swell PET substrates.

Figure 8 shows that large SWCNT bundles were welded, and small bundles were embedded on the PET substrate after spraying aromatic hydrocarbons, while spraying cyclohexane did not trigger welding. The strain induced on the SWCNT networks during network formation on the substrate may cause an initial high resistance in the SWCNT network film. Thus, solvent-induced chemical welding of the SWCNT film can release their strain. The recovery of the G band in the Raman spectra of the SWCNT films demonstrates strain relaxation via chemical welding.

Thermal treatment is an alternative way to produce SWCNT film-substrate welding without any chemicals. In particular, fast selective heating of CNTs on plastic substrates can provide an interesting opportunity for thermal welding [14, 15]. Microwaves irradiate the SWCNT films inside the rectangular waveguide microwave applicator, within which the microwave electric field is well defined and controlled. The microwave mode in the applicator is a

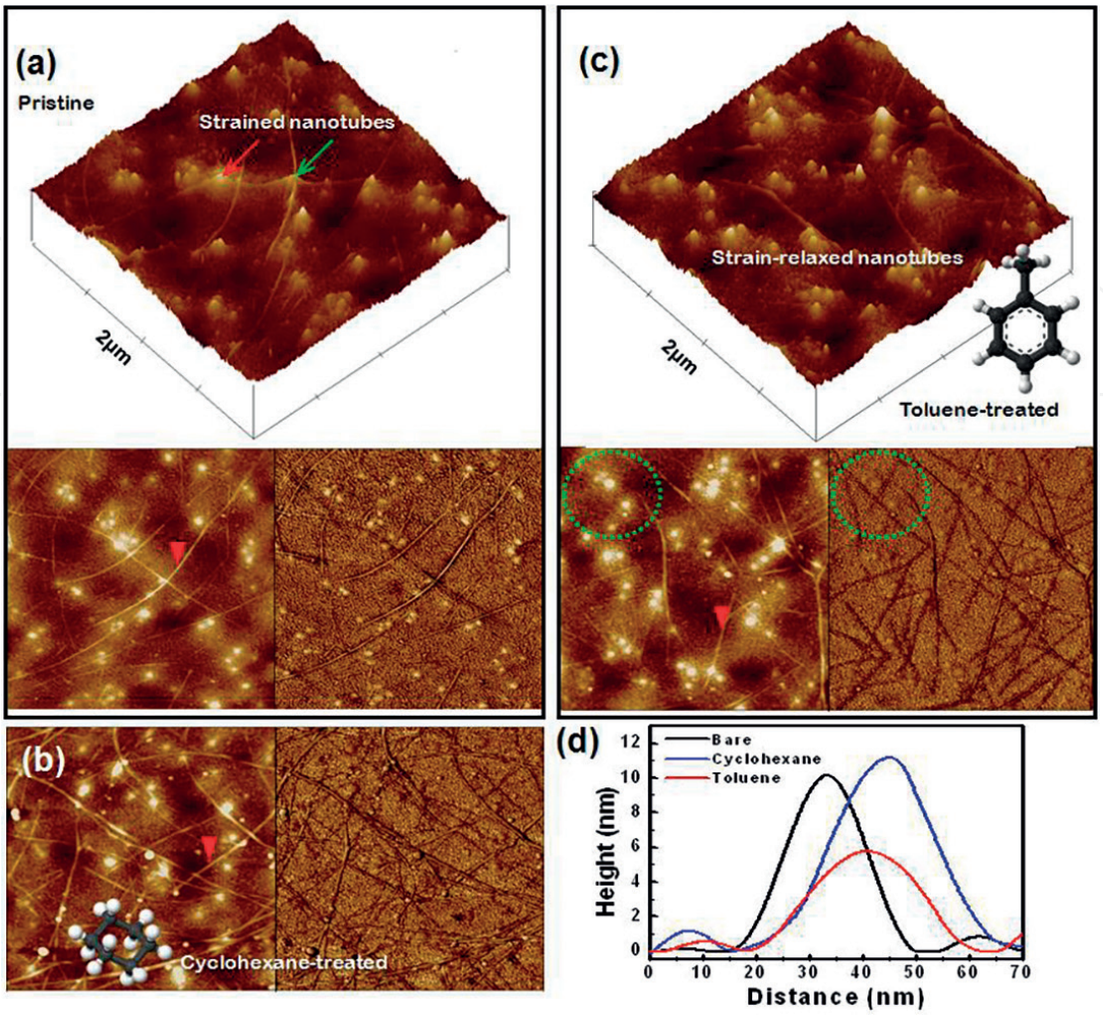

Figure 8. Atomic force microscope images of (a) an as-prepared film (99% transmittance at 550 nm), and the film after spraying of (b) cyclohexane and (c) toluene. (d) Height profile of the nanotube bundles indicated by the inverted triangles in (a–c). The left and right images in (a), (b), and (c) are the height and phase images, respectively. Deformed SWCNT bundles are indicated by arrows in (a). The green dotted circles in (c) indicate embedded SWCNT bundles after deposition of toluene because of swelling of PET [13].

fundamental transverse electric (TE_{10}) mode ($E_z = 0$) with a frequency of 2450 MHz, so the microwave electric field (E_y) is sinusoidally distributed along the x- and z-axes and constant along the y-axis. Immediate flash Ohmic heating with an energy conversion of greater than 99% can be realized because the microwave electric field is parallel to the overall SWCNT film and can efficiently induce a fast oscillating current in the film. The amplitude of the conduction current density, J_s, induced on the CNT film by the microwave electric field intensity, E_{MW}, may be described as follows [16]:

$$J_s = \sigma_{CNT} E_{MW}, \tag{3}$$

where σ_{CNT} is the electric conductivity of the SWCNT film.

Figure 9a shows the surface temperature and R_s changes of the SWCNT film by varying the irradiation time. The surface temperature of the SWCNT film is dramatically increased after

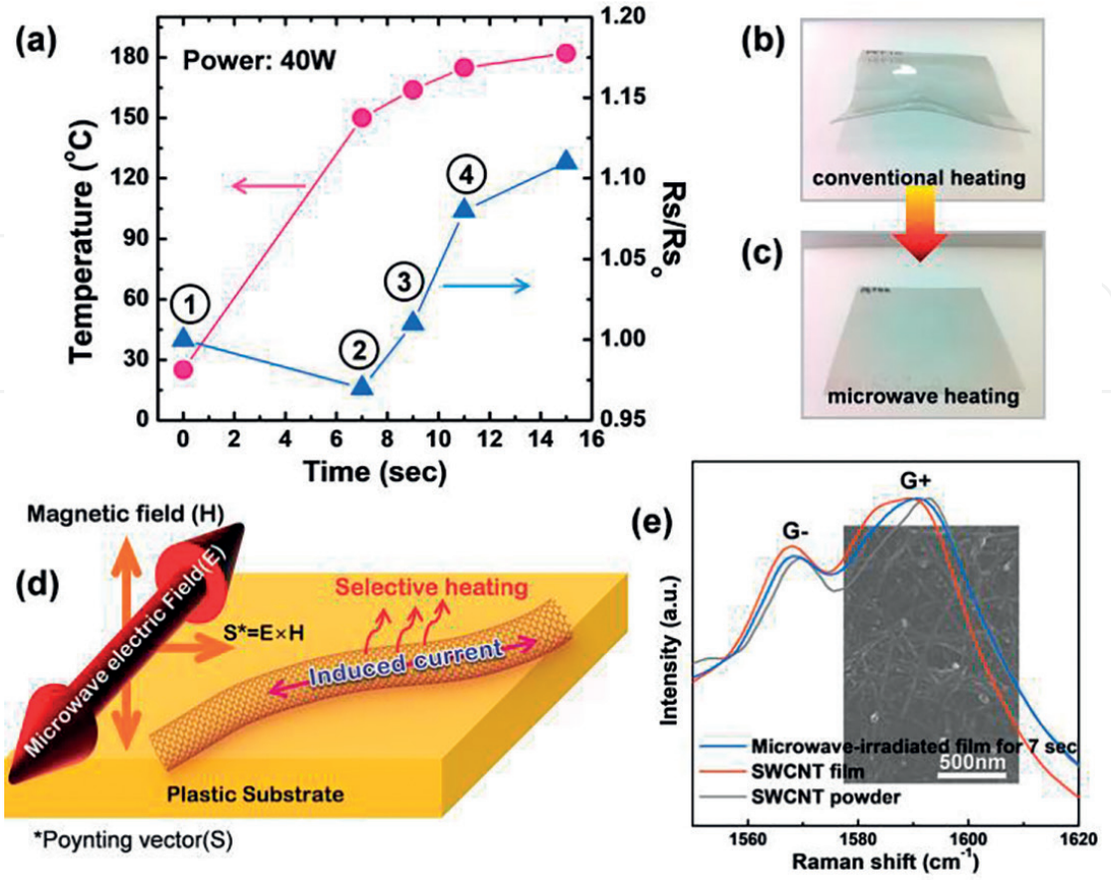

Figure 9. (a) Measured surface temperatures and R_s changes of SWCNT films on PC substrates as a function of microwave irradiation time. (b) The SWCNT film on PC heated in a conventional heating oven at 150°C. (c) The SWCNT film irradiated with microwaves. (d) Scheme of microwave-irradiated selective heating of CNTs on a plastic substrate, wherein a rapidly oscillating current induced along the CNTs is efficiently generated by the microwave electric field parallel to the SWCNT film. (e) Raman spectra of SWCNT powder and SWCNT films on PC before and after microwave irradiation for 7 s. Inset SEM image shows the microwave-nanowelded SWCNT film on the PC substrate [17].

7 s irradiation at 40 W without heat deflection. Of interest is that the R_s decreased after 7 s of irradiation, due to the occurrence of chemical welding. The Raman spectra in **Figure 9e** show the strain relaxation of the SWCNT network. The SEM image also shows clearly that the SWCNTs are welded or embedded in the plastic substrate. Importantly, the MW-irradiated SWCNT networks are protected by a self-passivation layer that protects the nanotubes from water molecules. The R_s values of the SWCNT films increase by less than 10% at 80°C and 90% relative humidity, despite embedding of the nanotubes in the plastic substrates.

3.3. CNT-induced migration of AgNW networks into plastic substrates

AgNW-based TCFs are not very environmentally stable without some form of passivation. If the AgNW network can be welded onto a thermoplastic substrate, it can be self-passivated, as was accomplished with SWCNT film. However, the surface tension of AgNWs (~500 mN/m of liquid silver in air) is much different from that of the hydrophobic PC substrate (~34.2 mN/m), which prevents the AgNWs from completely embedding in the plastic substrate, as illustrated in **Figure 10**. This surface tension mismatch can be solved by deposition of SWCNTs onto

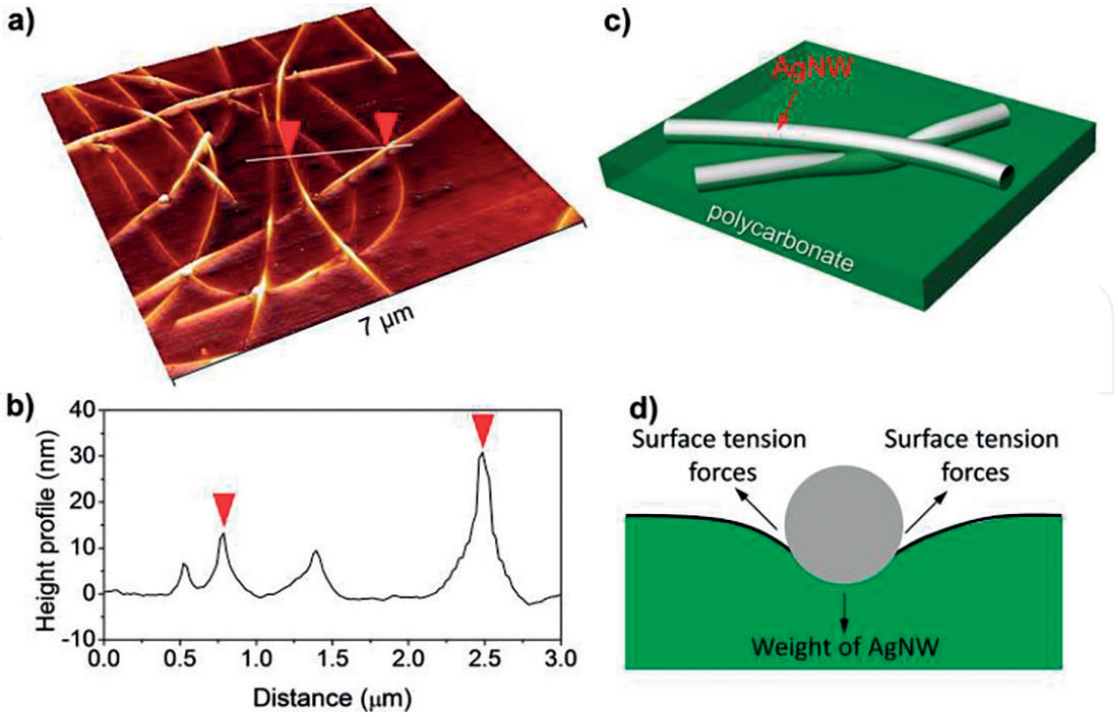

Figure 10. (a) AFM image and (b) height profile of the AgNW film after thermal treatment at 150°C for 3 h on a PC substrate. (c, d) Schematic illustration of the limited migration of AgNW networks into the plastic substrate due to a surface tension mismatch [18].

the AgNW network because of the low surface tension of CNTs (40–80 mN/m). Therefore, SWCNTs can trigger the migration of AgNWs into plastic substrates by thermal or chemical treatment. Moreover, the high thermal electrical conductivity of the SWCNT can promote the self-passivation of AgNWs by stable Joule heating of the film with an applied DC voltage. **Figure 11** shows the surface morphology of the SWCNT-overcoated AgNW film after a voltage of 20 V was applied. In stark contrast to AgNWs in AgNW film shown in **Figure 10a**, AgNWs were fully embedded in the plastic substrate by electrical heating. Atomic force microscopy (AFM) height profiles also demonstrate the embedding of the AgNW–SWCNT network in the plastic substrate. This self-passivation of AgNW networks assisted by SWCNTs with electrical heating improved the mechanical and hydrothermal stability of the film.

3.4. Interfacial engineering with GO for AgNW TCFs

In terms of the applications of metal nanowire networks, interfacial engineering is an important step to improve their performance with respect to electrical conductivity, environmental stability, surface roughness, and work function modulation. In particular, interfacial engineering of AgNW film can affect the opto-electrical performance because of junction formation in the network. In this study, HOGO nanosheets were utilized for efficient thermal joining of AgNW networks on thermoplastic substrates (**Figure 12a**). **Figure 12b** shows the R_s changes of the AgNW network films on bare PC, GO-modified PC, and glass after heating at 150°C with increasing exposure time. The R_s was dramatically reduced by thermal treatment via a junction joining of the networks. Importantly, the R_s decrease of the AgNW film was

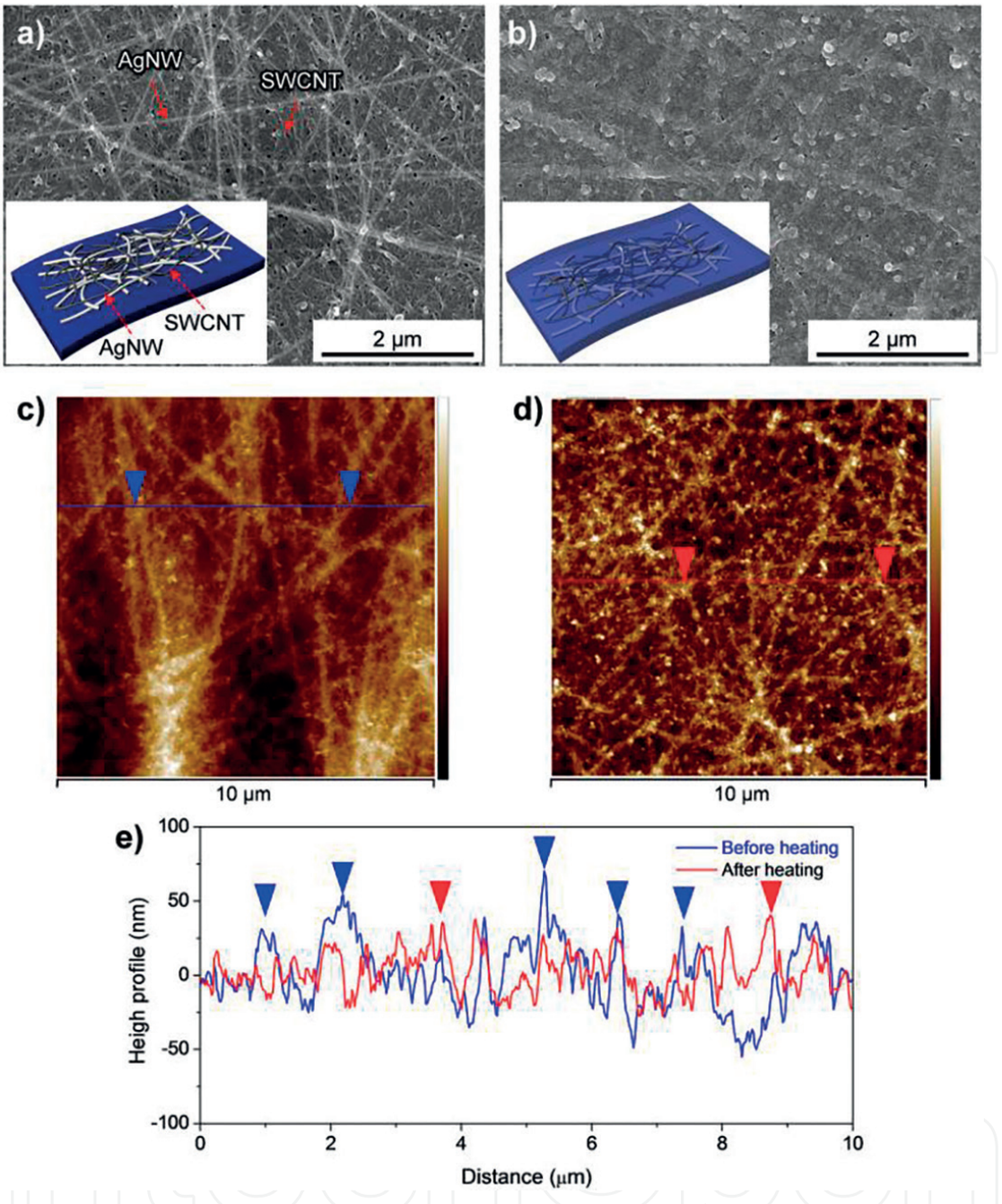

Figure 11. Field emission SEM images of AgNW overcoated with SWCNTs (a) before and (b) after heating under a current flow of thin film heater. AFM images of the same film (c) before heating and (d) after heating. (e) Height profile of the SWCNT-overcoated AgNW film under a current flow [18].

more efficient on GO-modified PC than on bare PC and glass. Interestingly, the changed R_s of AgNW films on PC was stable even after heating for 180 min, while the R_s of the AgNW film on glass gradually increased, even after 30 min, due to air oxidation. This result provides an opportunity to obtain high-performance AgNW TCFs by a combination of thermal welding and junction joining of AgNW networks. SEM and AFM images in **Figure 12** show clearly that on GO nanosheets, limited embedding or welding of AgNWs was observed. This demonstrates the more efficient reduction of R_s of AgNWs on the GO-modified PC.

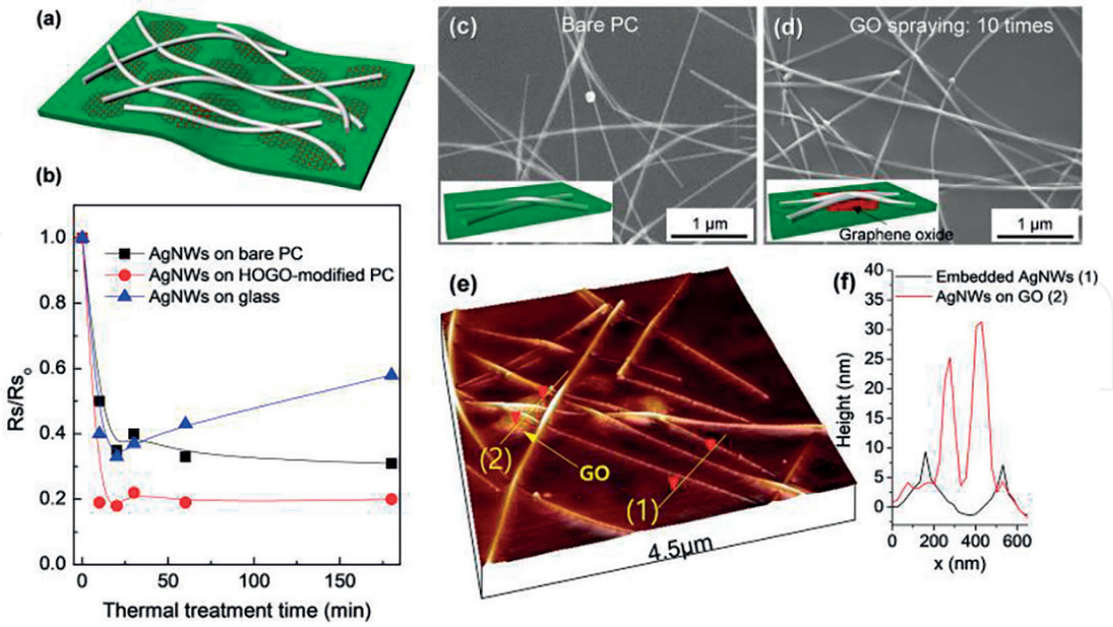

Figure 12. (a) Scheme showing AgNW film on GO-modified PC. (b) R_s changes of AgNW films on bare PC and GO-modified PC, and on glass after heating at 150°C by varying the exposure time. (c, d) SEM images of AgNW films on (c) bare PC and (d) GO-modified PC substrates after heating at 150°C for 1 h. (e) AFM image of AgNW networks on GO-modified PC. (f) Height profiles of embedded AgNWs and AgNWs floated on the GO nanosheet indicated in (e) as numbers [19].

4. High-performance TCFs by hybridization of 1D or 2D materials

4.1. Graphene oxide-modified SWCNT-based TCFs

SWCNT-based TCFs with a low haze value are suitable for highly transparent opto-electronic devices. However, for achievement of a low R_s value of the films, one challenge is the development of an efficient and stable dopant. In addition, their high porosity and hydrophobic surface properties are a drawback as an electrode material in opto-electronic devices. In this context, we introduced easily deformable GO nanosheets containing electron-withdrawing groups on the basal plane and edges, which can give a p-type doping effect on the SWCNT film. **Figure 13** shows that the R_s of the SWCNT film can be dramatically reduced by up to 40% compared to the as-prepared SWCNT film by deposition of GO solution onto the film by spraying. The efficiency of R_s reduction depends on the lateral sizes of the GO nanosheets. Small-sized GO nanosheets prepared by decanting the first supernatant (S1) by centrifugation were more efficient than larger GO nanosheets. As shown in **Figure 14**, the SWCNT bundles are easily wrapped with small GO nanosheets, while larger GO nanosheets can be freestanding between SWCNT networks. This means that densification of the SWCNT network is more efficient using small GO than large GO. The reduction of porosity and junction resistance of the SWCNT network can have a positive effect on the decrease of R_s. Moreover, the effect of p-type doping by GO is clearly shown in Raman spectra (**Figure 14c** and **d**). An upshift of 3.5 cm^{-1} in the G+ band for the semiconducting SWCNTs by small GO nanosheets (S1) demonstrates p-type doping of the SWCNTs from the GO nanosheets via a charge transfer mechanism.

To evaluate the opto-electrical performance of a GO-SWCNT electrode on PET, organic photovoltaic (OPV) cells with a PET/GO-SWCNT/PEDOT-PSS/active layer/LiF/Al structure were

http://dx.doi.org/10.5772/intechopen.80259

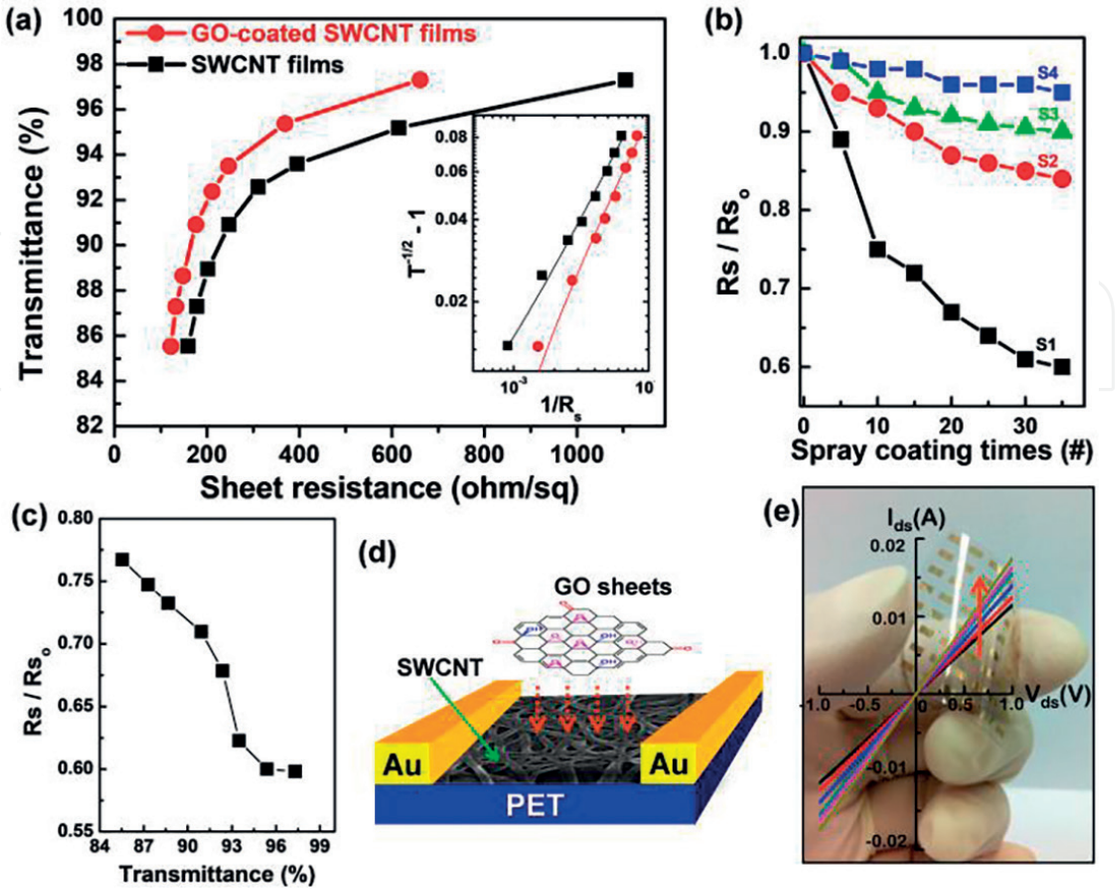

Figure 13. (a) R_s versus transmittance plots of SWCNT films before and after deposition of GO nanosheets. (b) Relative R_s changes of SWCNT films by increasing the number of spray coatings of GO solution obtained by centrifugation (the first to fourth supernatant solutions are denoted as S1 to S4). (c) Relative R_s as a function of the SWCNT film transmittance showing thickness dependence of GO deposition on R_s changes of the film due to contact area change between GO and the SWCNT bundle. (d) The I-V measurement scheme performed on SWCNT films after deposition of the GO solution. (e) Photo image of a gold-patterned SWCNT film and I-V plots for SWCNT films by increasing the amount of deposited GO solution (in the direction of the arrow) [20].

fabricated (**Figure 15**). For fabrication of the layered structure of the OPV cells, the wettability of the electrode on the upper loaded aqueous PEDOT:PSS solution is important. As shown in **Figure 15a**, the hydrophobic SWCNT film was converted to hydrophilic by deposition of hydrophilic GO nanosheets. Moreover, importantly, the work function of the SWCNT film changed from 4.7 to 5.05 eV by deposition of S1-GO nanosheets, which induces a facile hole injection from the HOMO of P3HT (5.0 eV) to the electrode. The resultant device performance with the GO-modified SWCNT anodes shows a significant enhancement in overall photovoltaic performance compared to devices fabricated on pristine SWCNT electrodes, as shown in **Figure 15d**.

4.2. Electrically stable SWCNT/AgNW hybrid TCFs

Under high current flow, metal NW scan be disrupted by Joule heating at the junction due to a relatively high junction resistance between metal NWs. Self-joining of NW network junctions can solve this problem via post-treatment. Another approach is to interconnect the NWs with other conducting materials or metal oxides. For more efficient processing of metal NW-based TCFs, we need to exclude additional steps, such as irradiation with light, heating at high

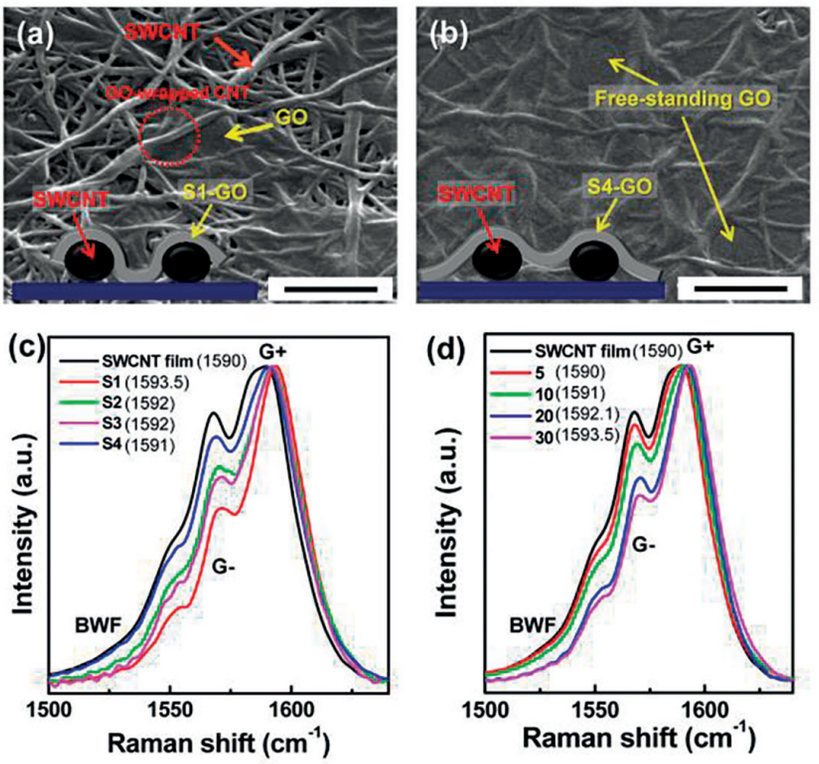

Figure 14. Tilted SEM images of SWCNT surfaces coated with (a) S1-GO nanosheets and (b) S4-GO nanosheets. Inset schemes show the structure of the GO-coated SWCNT networks. (c) Raman spectra of a pristine SWCNT film and films coated with S1, S2, S3, and S4 using a spray-coater 20 times. (d) Raman spectra of SWCNT films coated with S1-GO by increasing the number of coating layers from 5 to 30. Values in brackets in (c) and (d) indicate G+ band position. Scale bars in (a) and (b) are 300 nm [20].

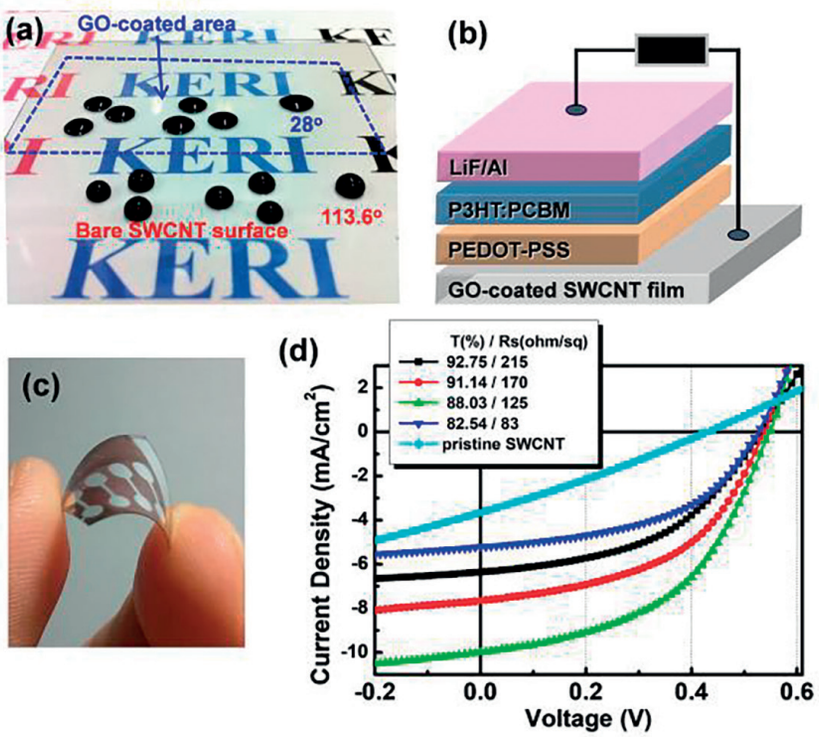

Figure 15. (a) PEDOT:PSS solution drop images on a, b are SWCNT surface and on the GO-coated area (dotted area). (b) Schematic structure and (c) photo image of OPV cell. (d) Current density (J) versus voltage (V) characteristics of pristine SWCNTs and GO-modified SWCNT photovoltaic cells under 100 mW/cm^2 AM 1.5G spectral illumination at various transmittance and R_s values [20].

temperatures, and the removal of surfactant molecules after the deposition of AgNWs or AgNW hybrid materials. Thus, we suggest that a small amount of SWCNTs can stabilize the AgNW networks under current flow without post-treatment. To realize this, the major challenge is the fabrication of a stable dispersion of SWCNTs in liquid medium without dispersant molecules that can be removed after deposition. To solve this issue, the SWCNTs were functionalized with quadruple hydrogen bonding (QHB) motifs of 2-ureido-4[1H]pyrimidinone (UHP) moieties through a previously reported sequential coupling reaction [21]. The AgNW/SWCNT mixture solution was easily prepared by direct mixing of the aqueous AgNW solution with a paste of SWCNTs functionalized with UHP (UHP-SWCNTs) by shaking, as shown in **Figure 16a**. The spray-coated AgNW/SWCNT hybrid film has an R_s value of ~20 Ω/sq. and $T > 90\%$ and was used to fabricate transparent film heaters to investigate the effect of SWCNTs on the electrical stability of the AgNW films under current flow. Notably, the breaking up of AgNWs at junctions was observed at 9 V (**Figure 17a**), which might have been induced by rapid joule heating at the junctions because of the high junction resistance of the AgNWs ($R_{11} \approx 10^3$–10^9 Ω). In stark contrast, after hybridization with SWCNTs, a new current pathway through the AgNW-SWCNT junction may be formed because of the relatively low contact resistance between the AgNW and SWCNT ($R_{12} \approx 10^3$ Ω) when compared to R_{11}, resulting in the formation of stable network films even at 15 V. Moreover, a very small work function difference between AgNW and UHP-SWCNTs, based on the Φ values of AgNW (4.1 eV) and UHP-SWCNTs (4.3 eV), can promote the current pathway through the AgNW-SWCNT junction (**Figure 18**).

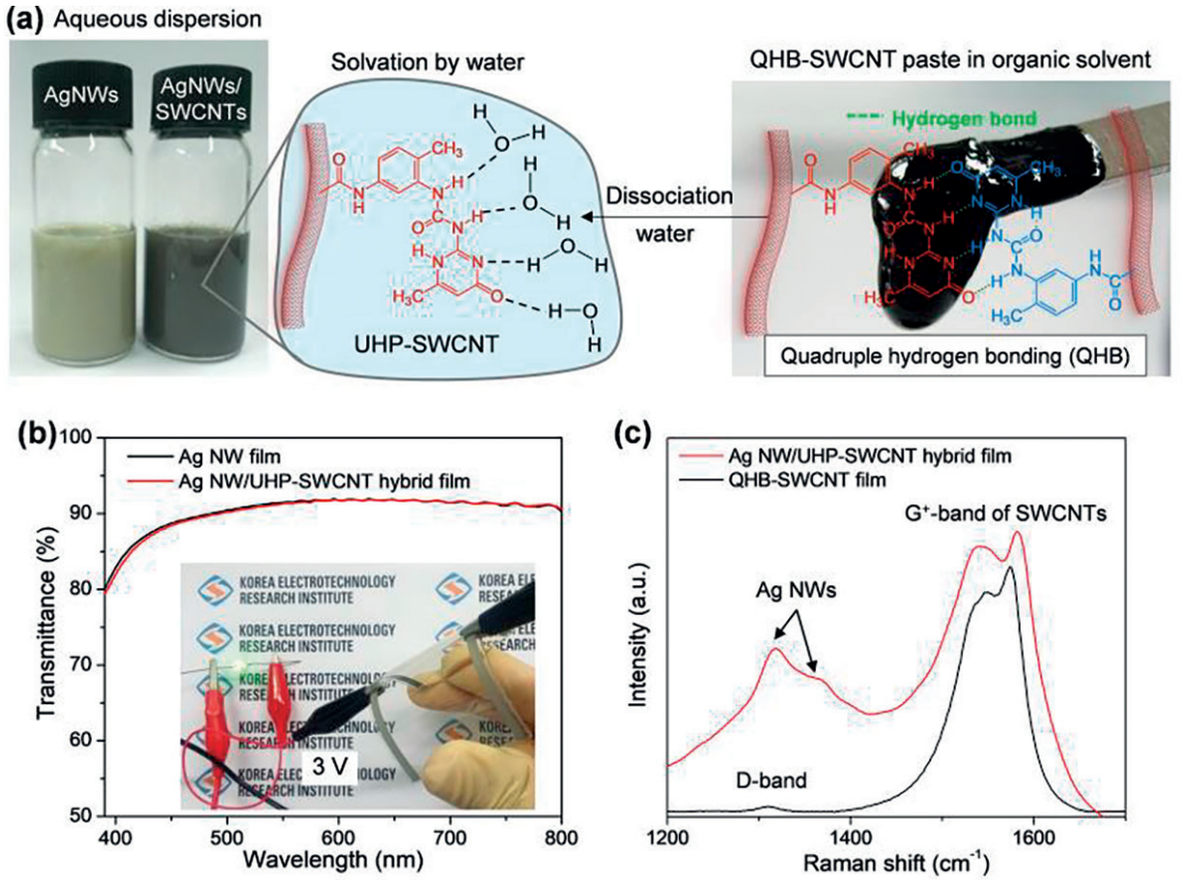

Figure 16. (a) Preparation of AgNW/SWCNT solution by direct mixing of aqueous AgNW solution and UHP-functionalized SWCNTs. (b) Optical transmission of the AgNW and AgNW/SWCNT hybrid films with $R_s \approx 20$ ohm/sq. fabricated by spraying. Inset image shows the lighting of an LED lamp at 3 V on bendable AgNW/SWCNT hybrid film on a polycarbonate substrate. (c) Raman spectra of the QHB-SWCNT film prepared by paste and AgNW/UHP-SWCNT hybrid films fabricated by mixture inks [22].

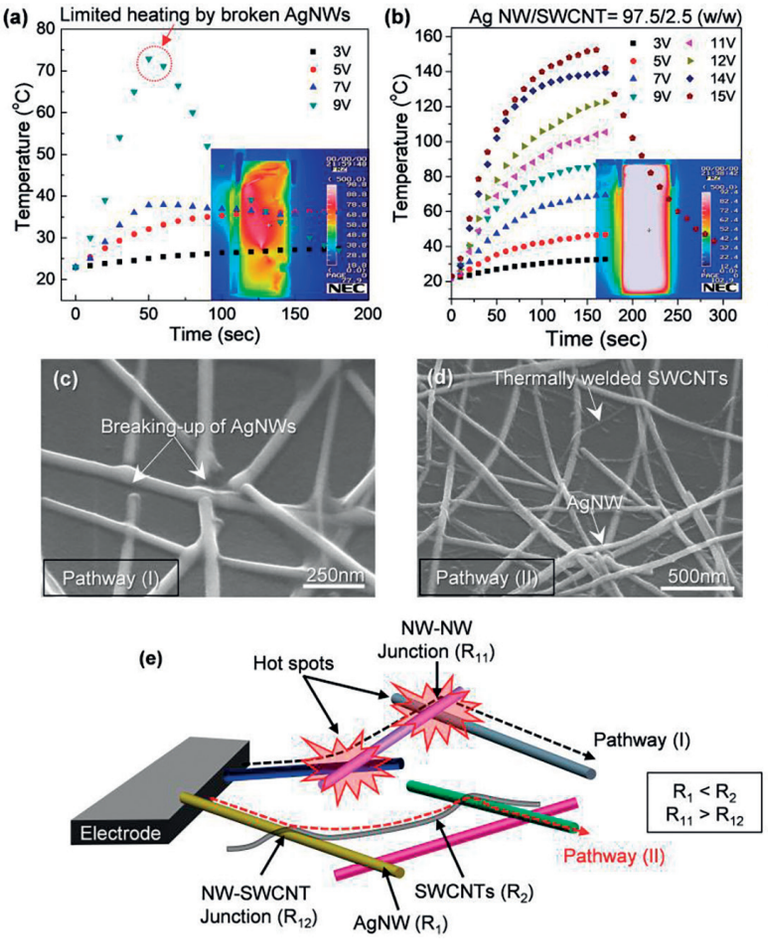

Figure 17. (a, b) Time-dependent temperature profiles of (a) AgNW and (b) AgNW/SWCNT hybrid films. The inset images are infrared thermal images of the film heaters. (c, d) Tilted SEM images of (c) AgNW and (d) AgNW/SWCNT hybrid films after heating at an input voltage of 9 V. (e) Schematic of AgNW/SWCNT hybrid networks showing possible current flow pathways (I, II). R1 and R2 indicate the resistivity of AgNWs and SWCNTs, respectively. R11 or R12 indicate the contact resistances between AgNWs or between AgNW and SWCNTs.

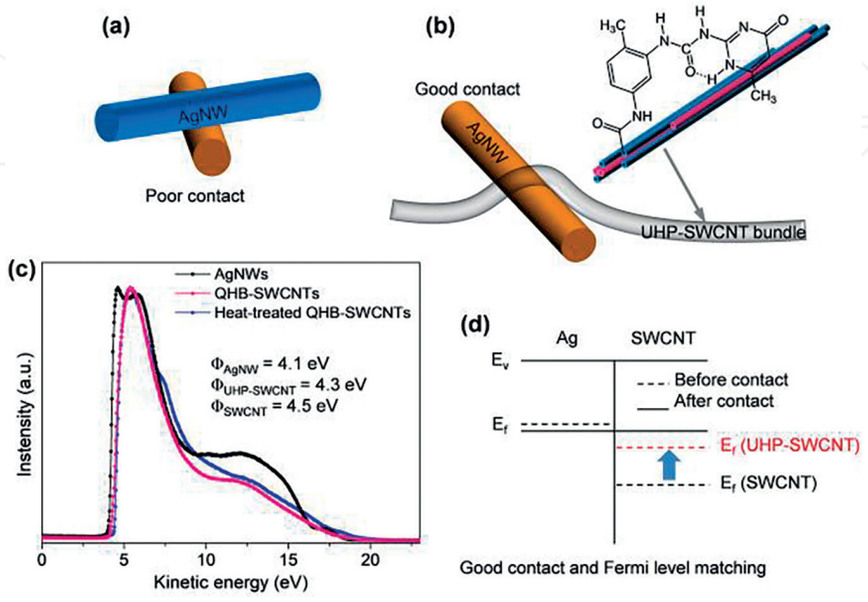

Figure 18. (a, b) Schematic diagram showing poor contact between AgNWs (a) and good contact between AgNW and UHP-SWCNTs. (c) Ultraviolet photoelectron spectroscopy spectra of AgNW, UHP-SWCNT, and thermally treated UHP-SWCNT films. (d) Schematic showing the reason for the current pathway through SWCNTs in terms of the work function.

5. Summary

We have briefly reviewed recent research progress on TCF technologies based on SWCNTs, AgNWs, and GO nanosheets via interfacial engineering and hybridization strategies. One-dimensional (1D) conducting nanomaterials such as CNTs and metal nanowires have been studied intensively because of their fascinating properties and offer tremendous potential for flexible opto-electronic applications in touch screen panels, flexible displays, solar cells, thin film heaters, signage, etc. To realize these applications, we need to develop high-performance TCFs with flexibility using a low-temperature process with scalable processing techniques on flexible plastic substrates. In this chapter, therefore, a scalable spray coating process using SWCNTs and AgNW solutions was introduced by demonstrating the wettability of the solution on surface energy-controlled substrates. One of the most important strategies for high-performance TCFs is interfacial engineering. Matching the interfacial tension between top-coating materials and the film is an important practical concept for fabrication of passivated TCFs that are environmentally stable at high humidity and temperature, as well as to improve their opto-electrical properties. Moreover, rational use of GO nanosheets and SWCNTs can improve AgNW network TCFs by welding in plastic substrates and efficient junction joining of AgNW junctions. Chemical or thermal welding of SWCNT networks is also useful for self-passivation of films on thermoplastic substrates.

In addition, recently developed AgNW/SWCNT hybrid TCF technologies can be commercially used to fabricate large area flexible TCFs by a roll-to-roll process because of fabrication of coating solutions without additional dispersant molecules.

For large opto-electronic devices with flexibility and stretchability, there are still many challenging issues for commercial application, including newly designed anisotropic conducting materials and their solution processing.

Acknowledgements

This work was supported by the Center for Advanced Soft-Electronics as Global Frontier Project (2014M3A6A5060953) funded by the Ministry of Science, ICT and Future Planning and by the Primary Research Program (18-12-N0101-18) of the Korea Electrotechnology Research Institute.

Author details

Joong Tark Han* and Geon-Woong Lee

*Address all correspondence to: jthan@keri.re.kr

Korea Electrotechnology Research Institute, Republic of Korea

References

[1] Ye S, Rathmell AR, Chen Z, Stewart IE, Wiley BJ. Metal nanowire networks: The next generation of transparent conductors. Advanced Materials. 2014;**26**:6670-6687. DOI: 10.1002/adma.201402710

[2] Kim Y, Ryu TI, Ok K-H, Kwak M-G, Park S, Park N-G, Han CJ, Kim BS, Ko MJ, Son HJ, Kim J-W. Inverted layer-by-layer fabrication of an ultraflexible and transparent Ag nanowire/conductive polymer composite electrode for use in high-performance organic solar cell. Advanced Functional Materials. 2015;**25**:4580-4589. DOI: 10.1002/adfm.201501046

[3] Xu F, Wu M-Y, Safron NS, Roy SS, Jacobberger RM, Bindl DJ, Seo J-H, Chang T-H, Ma Z, Arnold MS. Highly stretchable carbon nanotube transistors with ion gel gate dielectrics. Nano Letters. 2014;**14**:682-686. DOI: 10.1021/nl403941a

[4] Jeong I, Chiba T, Delacou C, Guo Y, Kaskela A, Reynaud O, Kauppinen EI, Maruyama S, Matsuo Y. Single-walled carbon nanotube film as electrode in indium-free planar heterojunction perovskite solar cells: Investigation of electron-blocking layers and dopants. Nano Letters. 2015;**15**:6665-6671. DOI: 10.1021/acs.nanolett.5b02490

[5] Li Z, Boix PP, Xing G, Fu K, Kulkarni SA, Batabyal SK, Xu W, Cao A, Sum TC, Mathews N, Wong LH. Carbon nanotubes as an efficient hole collector for high voltage methylammonium lead bromide perovskite solar cells. Nanoscale. 2016;**8**:6352-6360. DOI: 10.1039/C5NR06177F

[6] Woo JS, Lee G-W, Park S-Y, Han JT. Realization of transparent conducting networks with high uniformity by spray deposition on flexible substrates. Thin Solid Films. 2017;**638**:367-370. DOI: 10.1016/j.tsf.2017.08.010

[7] Hu L, Hecht DS, Grüner G. Percolation in transparent and conducting carbon nanotube networks. Nano Letters. 2004;**4**:2513-2517. DOI: 10.1021/nl048435y

[8] Lyons PE, De S, Blighe F, Nicolosi V, Pereira LFC, Ferreira MS, Coleman JN. The relationship between network morphology and conductivity in nanotube films. Journal of Applied Physics. 2008;**104**:044302/1-0044302/8. DOI: 10.1063/1.2968437

[9] Hecht D, Hu LB, Grüner G. Conductivity scaling with bundle length and diameter in single walled carbon nanotube networks. Applied Physics Letters. 2006;**89**:13112/1-13112/3. DOI: 10.1063/1.2356999

[10] Simien D, Fagan JA, Luo W, Douglas JF, Migler K, Obrzut J. Influence of nanotube length on the optical and conductivity properties of thin single-wall carbon nanotube networks. ACS Nano. 2008;**2**:1879-1884. DOI: 10.1021/nn800376x

[11] Nirmalraj PN, Lyons PE, De S, Coleman JN, Boland JJ. Electrical connectivity in single-walled carbon nanotube networks. Nano Letters. 2009;**9**:3890-3895

[12] Han JT, Kim JS, Jeong HD, Jeong HJ, Jeong SY, Lee G-W. Modulating conductivity, environmental stability of transparent conducting nanotube films on flexible substrates by interfacial engineering. ACS Nano. 2010;**4**:4551-4558

[13] Han JT, Kim JS, Lee SG, Bong H, Jeong HJ, Jeong SY, Cho K, Lee G-W. Chemical strain-relaxation of single-walled carbon nanotubes on plastic substrates for enhanced conductivity. Journal of Physical Chemistry C. 2011;**115**:22251-22256. DOI: 10.1021/nl9020914

[14] Imholt TJ, Dyke CA, Hasslacher B, Perez JM, Price DW, Roberts JA, Scott JB, Wadhawan A, Ye Z, Tour JM. Nanotubes in microwave fields: Light emission, intense heat, outgassing, and reconstruction. Chemistry of Materials. 2003;**15**:3969-3970. DOI: 10.1021/cm034530g

[15] Ye Z, Deering WD, Krokhin A, Roberts JA. Microwave absorption by an array of carbon nanotubes: A phenomenological model. Physical Review B. 2006;**74**:075425. DOI: 10.1103/PhysRevB.74.075425

[16] Metaxas AC, Meredith RJ. Industrial Microwave Heating. London: Peter Peregrinus Ltd.; 1988. ISBN-0-906048-89-3

[17] Han JT, Kim D, Kim JS, Seol SK, Jeong SY, Jeong HJ, Chang WS, Lee G-W, Jung S. Self-passivation of transparent single-walled carbon nanotube films on plastic substrates by microwave-induced rapid nanowelding. Applied Physics Letters. 2012;**100**:163120/1-163120/4. DOI: 10.1063/1.4704666

[18] Woo JS, Kim BK, Kim HY, Lee G-W, Park SY, Han JT. Carbon nanotube-induced migration of silver nanowire networks into plastic substrates via Joule heating for high stability. RSC Advances. 2016;**6**:86395-86400. DOI: 10.1039/C6RA17771A

[19] Woo JS, Sin DH, Kim H, Jang JI, Kim HY, Lee G-W, Cho K, Park S-Y, Han JT. Enhanced transparent conducting networks on plastic substrates modified with highly oxidized graphene oxide nanosheets. Nanoscale. 2016;**8**:6693-6699. DOI: 10.1039/C5NR08687F

[20] Han JT, Kim JS, Jo SB, Kim SH, Kim JS, Kang B, Jeong HJ, Jeong SY, Cho K, Lee G-W. Graphene oxide as a multi-functional p-dopant of transparent single-walled carbon nanotube films for optoelectronic devices. Nanoscale. 2012;**4**:7735-7742. DOI: 10.1039/C2NR31923C

[21] Han JT, Jeong BH, Seo SH, Roh KC, Kim S, Choi S, Woo JS, Kim HY, Jang JI, Shin D-C, Jeong S, Jeong HJ, Jeong SY, Lee G-W. Dispersant-free conducting pastes for flexible and printed nanocarbon electrodes. Nature Communications. 2013;**4**:2491. DOI: 10.1038/ncomms3491

[22] Woo JS, Han JT, Jung S, Jang JI, Kim HY, Jeong HJ, Jeong SY, Baeg K-J, Lee G-W. Electrically robust metal nanowire network formation by in-situ interconnection with single-walled carbon nanotubes. Scientific Reports. 2014;**4**:4804. DOI: 10.1038/srep04804

IntechOpen